Curvelet Transform with Adaptive Tiling

Hasan Al-Marzouqi and Ghassan AlRegib
School of Electrical and Computer Engineering
Georgia Institute of Technology, Atlanta, GA, 30332-0250
{almarzouqi, alregib}@gatech.edu

ABSTRACT

The curvelet transform is a recently introduced non-adaptive multi-scale transform that have gained popularity in the image processing field. In this paper, we study the effect of customized tiling of frequency content in the curvelet transform. Specifically, we investigate the effect of the size of the coarsest level and its relationship to denoising performance. Based on the observed behavior, we introduce an algorithm to automatically choose the optimal number of decompositions. Its performance shows a clear advantage, in denoising applications, when compared to default curvelet decomposition. We also examine how denoising is affected by varying the number of divisions per scale.

Keywords: image processing, curvelet transform, denoising, transform theory, wavelet extension.

1. INTRODUCTION

Since their introduction in the last decade [1, 2, 3, 4], the curvelet transform demonstrated successful performance improvement in a wide range of application areas including denoising [5, 6], image fusion and inpainting [7], edge enhancement [8], and feature detection [9, 10]. This wide-spread use is linked to curvelets approach in capturing edge information in images. Interesting features in images are usually represented by edges. The multi-scale orientation sensitive frequency domain tiling as presented in the curvelet transform, is proven to be very efficient in handling edges. Fig. 1 shows the curvelet original frequency domain tiling. In this figure we notice the use of different scales where each scale is divided into a number of wedges that increase as we move outward towards the image boundary. In this paper we extend this edge-efficient representation by allowing adaptive tiling of the frequency domain. In this method the tiling of frequency content is dependent on the frequency content of a specific image or a collection of images representing a class of interest. The remainder of this paper is organized as follows. In the next section an overview of the curvelet transform is presented. In section three we derive an algorithm to find the optimal number of decomposition scales using frequency content. Its improved performance is demonstrated on a number of test cases. In Section 4 we present the results of adapting the number of divisions used per scale along with the corresponding denoising performance. Conclusions and directions for future research are given in section 5.

2. THE CURVELET TRANSFORM

The curvelet transform of a given image can be describes as a set of coefficients given by the following relationship:

$$c(j,l,k) = \int f(w) U_{j,l}\left(S_{\theta l}^{-1} w\right) e^{i\langle b,w\rangle} dw \qquad (1)$$

Where *c(j,l,k)* is the curvelet coefficient at scale *j*, wedge location *l*, and coordinates k=(k1,k2) $\in \mathbf{Z}^2$. The distribution of scales and locations is shown in fig 1. This pseudopolar dyadic tiling was used successfully

Image Processing: Algorithms and Systems X; and Parallel Processing for Imaging Applications II, edited by Karen O. Egiazarian, Sos S. Agaian, Atanas P. Gotchev, John Recker, Gujin Wang, Proc. of SPIE-IS&T Electronic Imaging, SPIE Vol. 8295, 82950F • © 2012 SPIE-IS&T • CCC code: 0277-786X/12/$18 • doi: 10.1117/12.909111

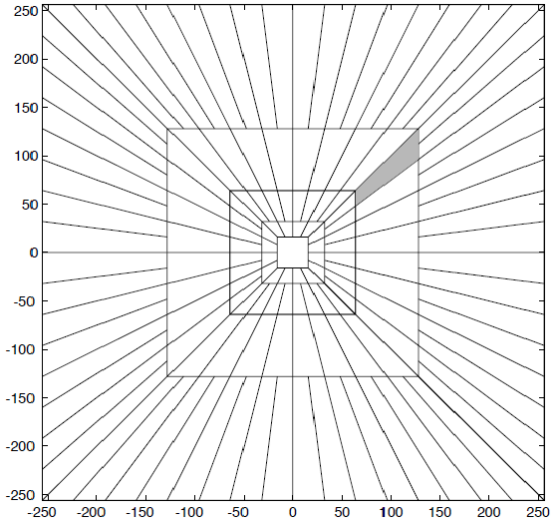

Fig. 1: The pseudopolar tiling of the frequency domain. Shaded region represents a typical wedge

with wavelets and other harmonic analysis algorithms [11],[12]. *f(w)* is the FFT value at *w*. $S_\theta := \begin{pmatrix} 1 & 0 \\ -\tan\theta & 1 \end{pmatrix}$ is the shear matrix. $\theta \in \left[-\frac{\pi}{4}, \frac{\pi}{4}\right]$. $U_{j,l}$ is a localizing smoothing window. $b \approx (k_1\, 2^{-j}, k_2\, 2^{-j/2})$. The following steps detail how such coefficients can be computed:

1. Find the 2D FFT of the desired image.
2. For each scale *j* and scale *l*, smooth the FFT values in each wedge by the smoothing window $U_{j,l}$. This prevents discontinuities and is necessary for prefect recovery. To prevent loss of energy, The functions $U_{j,l}$ also have to be constructed so that they overlap in a way that makes the squared sum of $U_{j,l}$ at each coordinate equal to one:

$$\sum_{\forall j}\sum_{\forall l}|U(j,l)|^2 = 1 \qquad (2)$$

3. Compute the inverse FFT to each wedge. Since the wedges do not correspond to rectangles, the inverse FFT is computed using the periodicity of the Fourier transform. Using periodicity one can tile the frequency domain with copies of the FFT values of the given wedge. The FFT is then computed for the values in the rectangle surrounding the origin.

The inverse transform is computed by reversing the above steps, which corresponds to:

1. Compute the 2D FFT for each scale *j* and location *l*.
2. Multiply each scale/location by the corresponding smoothing window. The smoothing window needs to be 'wrapped' to correspond to the new distribution of frequency values computed by step 3 in the forward transform.
3. The frequency values are mapped pack 'unwrapped' to their original scale/wedge location. Take the 2D inverse FFT, to get the original image back.

An alternative to the wrapping approach, in computing the FFT for curvelet wedges, is to rotate the coordinate system aligning it with the orientation of each wedge. In this case we have:

$$c(j,k,l) = \int f(S_{\theta l} w) U_j(w) e^{i<b,w>} dw \qquad (3)$$

The two implementations for curvelets are available online. The results presented in this paper are relevant to either one of them. However, due to its computational efficiency and to avoid interpolation artifacts the wrapping implementation is the approach investigated in this study.

Note from Figure 1, that the coarsest level (*j=1*) is not directional. Its effect is similar to a low pass filter. The corresponding coefficient values represent the smoothest areas in the image. The outer finest level is proposed to be either a non-directional wavelet or curvelets. Use of directional curvelets comes with higher computational cost, but always achieves better results. It's the option we chose for this study.

Using curvelets, the finest scale is a periodic extension of the original image. The ratio of the new size to the old one is fixed at $1.\overline{3}$. The number of scales *J* is determined by the size of the input image. The number of wedges per scale increases from the coarsest scale to the finest and is equal to 2^{2j} where *j=1, 2… J*. Although, that values of curvelet coefficients are completely determined by the frequency content, tiling of the frequency space takes the same dyadic approach with mostly fixed parameters. Naturally, adapting these divisions to correspond to the frequency content in the image will generate better performance results. In the next sections experimental results with two possible adaptations are presented.

3. OPTIMAL NUMBER OF SCALES

One important factor that is controlled by the number of scales *J* is the size of the coarsest level. As J increases, the size of the coarsest level becomes smaller. In the original curvelet implementation this parameter is either chosen by the user or defaulted to be dependent on the image size.

$$J = \lceil log_2(\min(N_1, N_2) - 3 \rceil \qquad (4)$$

Where $\lceil * \rceil$ is the smallest integer greater than or equal to *. N_1 and N_2 are the number of horizontal and vertical image pixels. Obviously, $\log_2$ corresponds to the dyadic scaling. Subtraction by one is necessary to find *J* needed to reach the origin of the frequency domain. Another two are subtracted to allow for a reasonable size coarsest level window (2^2=4).

Scanning a variety of natural images, one easily observes a region of relatively high magnitude coefficient values surrounding the origin of the frequency space (Figure 2). This region corresponds to continuous and relatively smooth areas in the image domain. Naturally, these areas are not directional. Use of curvelets in these regions is not necessary and could even lead to performance degradation. Thus, they can be used as an indicator of the optimal *J* value. The following algorithm is developed to detect the size of this region:

1. Define $mid\_range = \frac{\max(\log_{10}(\text{FFT coeff. magnitude})) + \min(\log_{10}(FFT\ coeff.magnidute))}{2}$ (5)
2. Let $D = D_{initial}$ =7 pixels. This insures a minimum coarsest window of size 7×7.
3. Set a square surrounding the origin of the frequency domain with a diagonal length equal to *D* pixels.
4. If more than 99% of the log-magnitudes of Fourier coefficients within the square are larger than the *mid_range* value then go to step 5. Otherwise set *D=D*-2, and exit the algorithm
5. Set *D=D+2* and return to stop 4.

The optimal number of scales is found using the side length of the square with diagonal *D* returned from step 4. Since the diagonal is measured using pixels, the coarsest level square found is of size *D×D*.

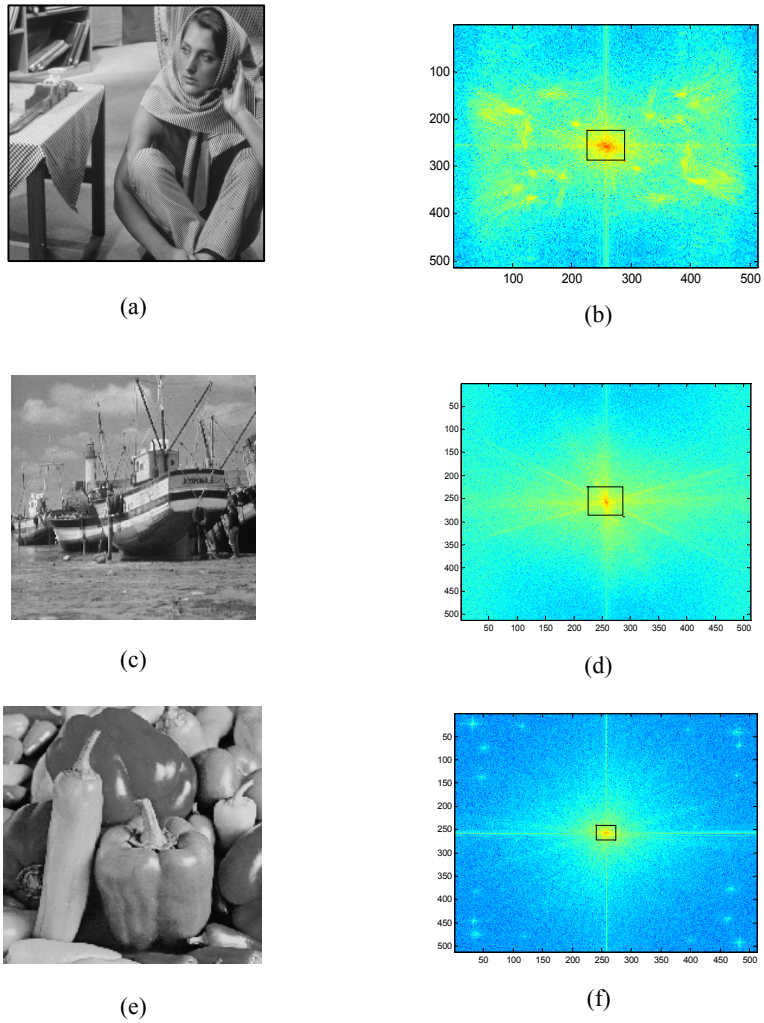

(a) (b) (c) (d) (e) (f)

Figure 2: Three images and a plot of their corresponding FFT magnitudes plotted in log-scale. The scale is increasing in value from blue to red. A high magnitude region is observed around the center of the frequency space. The black square shows the coarsest level region found by our scale selecting algorithm

Using dyadic scaling the optimal number of scales J is computed as follows.

$$\text{Optimal number of scale} = \lceil (log_2(\min(N_1, N_2)) - 1) - (log_2(D) - 1) \rceil \qquad (6)$$

$$= \lceil log_2(\min(N_1, N_2)) - log_2(D) \rceil$$

$$= \left\lceil log_2\left(\frac{\min(N1, N2)}{D}\right) \right\rceil \qquad (7)$$

Where equation (5) computes the difference between the number of scales needed to reach the origin of the frequency domain from the edge of the image, and the number of scales needed to reach the origin from the edge of the coarsest level square. $\lceil * \rceil$ is the smallest integer greater than or equal to *.

In order to test the above algorithm, optimal decomposition values were found for 6 test images. Zero-mean Gaussian noise with standard deviation σ=20 was added to each image. We used thresholding to denoise each

of these images. In each of the six test cases we used *J* number of decomposition levels as computed from the scale selecting algorithm. In all cases the results showed improvements in denoising performance. Table 1 demonstrates improved PSNR values compared with the default curvelet construction. The default curvelet results were found using default parameters values except for the use of curvelets at the finest scale. The new choice of *J* did also save time and memory requirements, since the number of optimal coefficients were often smaller than the ones found using the default curvelet construction.

4. FINDING OPTIMAL NUMBER OF DIVISIONS PER SCALE

In the original curvelet implementation the number of wedges per scale increases as we move outward to the image boundary. In our experiments, we tested denoising performance while varying the number of divisions in each scale. Since the FFT data are symmetric around the origin, two possible choices of wedges exist for each scale. The *2J* parameter values were varied from 4 to 32 in steps of 4. *J* was determined using the scale selecting algorithm presented in the previous section. Performance in denoising test images contaminated by Gaussian noise with standard deviation σ=20 was examined. Results show that denoising performance can be improved by allowing more flexibility on the choice of number of division per scale (Table 1). In real applications one can consider learning these optimal divisions per scale from a collection of training images representing the class of interest.

Table 1. Improvement in denoising additive Gaussian noise σ=20. Performance measured using PSNR. Improvements are relative to the original curvelet construction (default parameters + curvelets at finest level)

	Improvement due to the number of scales (db)	**Improvement due to optimal divisions per scale/quadrant (db)**	**Overall improvement (db)**
Barbara	0.273	0.031	0.304
Boats	0.155	0.075	0.230
Camera man	0.113	0.064	0.177
Lena	0.208	0.066	0.274
Peppers	0.173	0.107	0.280
Seismic	0.143	0.290	0.433

5. CONCLUSIONS AND VIEW OF FUTURE WORK

Results on adapting the construction of curvelet frequency domain tiling were discussed in this work. We have demonstrated that a clear progress in denoising performance can be achieved by choosing the appropriate number of scales and the suitable number of divisions per scale. An algorithm to choose the optimal number of scales was developed and its performance was validated on a number of test images. Even though transform capability was measured in terms of denoising performance, it is very likely that this advantage in denoising correspond to further improvements in other application areas such as edge enhancement and feature detection. Currently, we are considering further tiling adaptations. Finding analytical formulas to automate the choice of optimal values is another interesting research path to pursue. We are already observing signs of a quantifiable relationship between frequency content and the number of divisions per scale as illustrated in Figure 3.

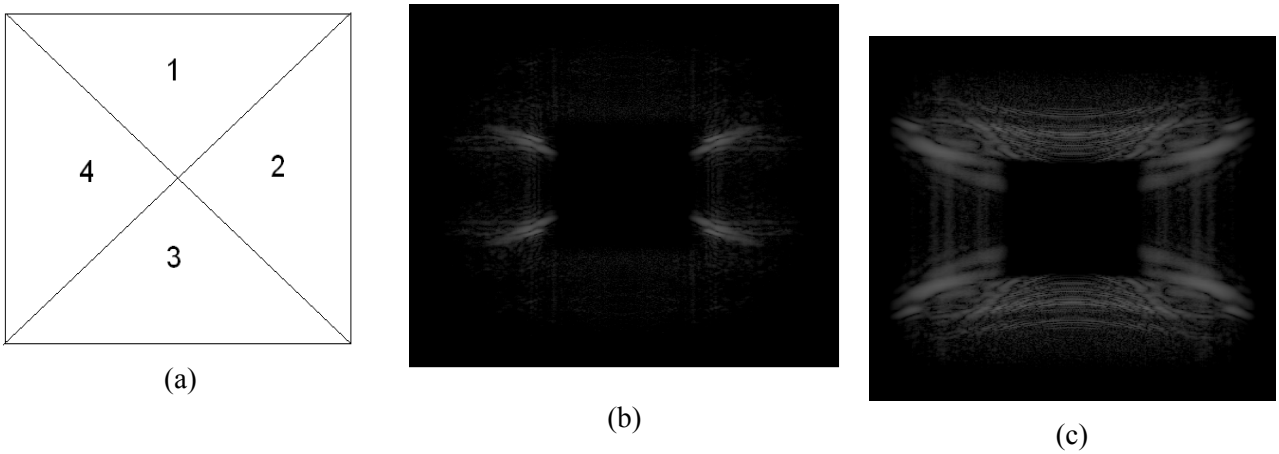

(a) (b) (c)

Fig. 3: Optimal number of division per scale and frequency content: (a) curvelet quadrant's (b) First scale frequency content of a seismic image: optimal values quadrants 1 and 3:4 divs. , quadrants 2 and 4: 12 divs. (c) Second scale frequency content of the same image: optimal values quadrants 1 and 3: 12 divs., quadrants 2 and 4: 4 divis.

REFERENCES

[1] Candes E, Donoho D. "New tight frames of curvelets and optimal representations of objects with piecewise C2 singularities". *Communications on pure and applied mathematics*. 57(2):219-266.

[2] Candès E, Demanet L, Donoho D, Ying L. "Fast Discrete Curvelet Transforms". Multiscale Modeling & Simulation. 2006;5(3):861.

[3] E. Candès and D. Donoho, "Continuous curvelet transform. I. Resolution of the wavefront set," Appl. Comput. Harmon. Anal., vol. 19, no. 2, pp. 162–197, 2005.

[4] Jianwei Ma; Plonka, G. , "The Curvelet Transform," Signal Processing Magazine, IEEE , vol.27, no.2, pp.118-133, March 2010 1.

[5] Starck J-L, Candès EJ, Donoho DL. "The curvelet transform for image denoising". *IEEE Transactions on image processing :* 2002;11(6):670-84.

[6] A. Federico and G. H. Kaufmann, "Denoising in digital speckle pattern interferometry using wave atoms", Opt. Lett. 32 (2007) 1232-1234

[7] Filippo Nencini, Andrea Garzelli, Stefano Baronti, and Luciano Alparone. 2007. "Remote sensing image fusion using the curvelet transform". *Inf. Fusion* 8, 2 (April 2007), 143-156.

[8] Starck, J.-L.; Murtagh, F.; Candes, E.J.; Donoho, D.L.; , "Gray and color image contrast enhancement by the curvelet transform," *Image Processing, IEEE Transactions on* , vol.12, no.6, pp. 706- 717, June 2003.

[9] A. A. Mohammed, R. Minhas, Q. M. Jonathan Wu, and M. A. Sid-Ahmed. 2011. "Human face recognition based on multidimensional PCA and extreme learning machine". *Pattern Recogn.* 44, 10-11 (October 2011), 2588-2597.

[10] Tanaya Mandal, Q.M. Jonathan Wu, Yuan Yuan, "Curvelet based face recognition via dimension reduction", Signal Processing, Volume 89, Issue 12, Special Section: Visual Information Analysis for Security, December 2009, Pages 2345-2353.

[11] M. N. Do. and M. Vetterli, "Contourlets", in *Beyond Wavelets*, G. V. Welland ed., Academic Press, 2003.

[12] A. G. Flesia, H. Hel-Or, A. Averbuch, E. J. Candes, R. R. Coifman and D. L. Donoho, "Digital implementation of ridgelet packets", *Beyond Wavelets*, J. Stoeckler and G. V. Welland eds., Academic Press, 2003.